POLITECNICO
MILANO 1863

SCUOLA DI INGEGNERIA INDUSTRIALE
E DELL'INFORMAZIONE

EXECUTIVE SUMMARY OF THE THESIS

# Towards OAM Light Generation with Femtosecond Laser Written Waveguides Circuits

TESI MAGISTRALE IN ENGINEERING PHYSICS – INGEGNERIA FISICA

**AUTHOR: OMER AHMED SIDDIG ALTAHER**

**ADVISOR: Dr. Roberto Osellame**

**ACADEMIC YEAR: 2021-2022**

## 1. Introduction

The ability to encode information in spatial degrees of freedom holds a considerable potential for a variety of applications, with a particular focus on the orbital angular momentum of classical and quantum light states. Such states form discrete high-dimensional quantum systems, also called qudits. A qudit is encoded on a quantum particle which is not limited to two states but in principle can have any number of discrete levels. As a result, the qudit enlarges the amount of information that a single quantum carrier can hold [1][2][3]. The fundamental property of photons carrying orbital angular momentum (OAM) is the presence of the helical phase factor $e^{il\varphi}$, where $\varphi$ is the azimuthal coordinate that is in the plane transverse to the propagation direction. OAM beams are typically produced using bulk optics components, which however are limited to shaping the wavefront of a free-space propagating light beam [4][5].
Interestingly, an OAM beam could be also produced exploiting the far-field distribution emitted by the output of an array of N waveguides, placed at the vertices of a regular polygon, endowed with a cyclical phase, as shown in ref [6]. The required integrated circuit to generate an optical beam possessing OAM in this scenario could be divided into three different sections. A power splitting device, such as a star coupler or a cascade of directional couplers, could be used in the first stage, to divide the input light from the fiber into several branches with the required amplitude ratios and cyclical phase terms. The phase terms of each waveguide could be possibly tuned, thus correcting the experimental imperfection, using an array of phase shifters (such as thermo-optic devices) in the second part [7]. A third section would transform the waveguides from a planar arrangement to the required two-dimensional cross-section, bringing each waveguide to its final position.

A powerful technique to realize photonic circuits is femtosecond laser written waveguiding (FLW). FLW is based on the non-linear absorption of focused laser pulses in the transparent material. This leads to a smooth and permanent

modification of the refractive index in correspondence of the focal spot (Figure 1) [8].
The three-dimensional capabilities of FLM enable the fabrication of arrays of single-mode waveguides placed at the vertices of a regular polygon structure. Moreover, the output mode of each waveguide is a nearly-gaussian mode.
This work provides the experimental demonstration of the third section of the device, which transforms eight waveguides from a planar configuration to the vertices of a regular octagonal cross-section using femtosecond laser micromachining (FLM). Good control is shown on the parasitic coupling among neighboring waveguides, in the region where they are brought close together to produce the final octagonal structure.

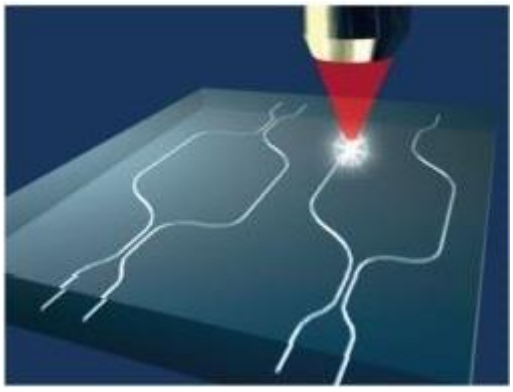

**Figure 1:** Femtosecond Laser Micromachining fabrication process on dielectric material [7].

## 2. Waveguide Optimization

Waveguide optimization involves in principle many inscription parameters. Here we concentrated on the writing velocity and beam irradiation power. These two factors are simple to manipulate and have been shown to be very effective in the literature. The values of the other parameters were instead taken from the literature, or from the research-group experience with the same substrate.
The pulse duration was set at 170 fs and the laser repetition rate was 1 MHz. Alumino-borosilicate glass samples that were 1±1 mm thick had waveguides fabricated onto them. Additionally, all waveguides were fabricated at a depth of 60 $\mu m$. This in fact would possibly boost the effectiveness of thermal phase-shifters, since waveguides need to be close to the surface in order to perform an efficient modulation of the refractive index and maintain low power dissipation [].

The use of the multi-pass approach, which employs numerous overlapped laser scans, allowed for the creation of waveguides with a larger index contrast. Additionally, this method enhances the waveguide confinement qualities, which is beneficial for achieving lower bending radii and more compact devices.

Numerous waveguides were fabricated with writing velocities ranging from 15 m/s to 30 mm/s, exploring a wide range of values for the irradiation power from 200 mW to 380 mW, and a fixed number of 6 overlapped scans. The straight waveguides are fabricated on 2-cm long sample of Eagle XG glass. Waveguide characterization is performed by coupling laser light at 808 nm wavelength with the so-called end-fire coupling setup, which is used for all the optical characterization. Measurements can evaluate the power distribution at the output ports. the values of the Insertion losses were measured (Figure 2), then also separated the distinct loss factors, with coupling losses (CL) and propagation losses (PL).

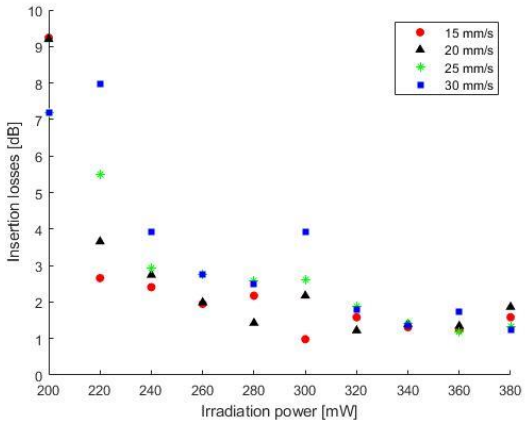


**Figure 2:** IL as function of the irradiation power for different writing velocities.

As a result, we chose as the optimal waveguides the ones fabricated at 340 mW since they have identical amounts of insertion losses 1.3 dB for all the writing velocities. CL evaluated via the overlap integral between the single-mode fiber's mode (780HP) and the written waveguides, are less than 0.1dB. Therefore, PLs 0.5 dB/cm were calculated for the waveguides using Eq (1), considering 0.035 dB as Fresnel Loss (FL):

$$PL|_{dB/cm} = \frac{IL - CL - 2FL}{L} \qquad (1)$$

Radiation losses, known as bending losses, result from the guiding path's curvature along the propagation direction.
To evaluate experimentally this loss contribution, we fabricated S-bends (two successive circular arcs producing an S-shaped waveguide) with bending radii varying from 15 mm to 90 mm, and several writing velocities. The same total curved length $L_s$ was kept for all waveguides. Additionally, straight waveguides were realized, enabling the reference measurement of $IL|_{SWG}$ and retrieval of the bending losses (BL) using Equation (2).

$$BL|_{dB/cm} = \frac{IL|_{SWG} - IL|_{BWG}}{L_s} \qquad (2)$$

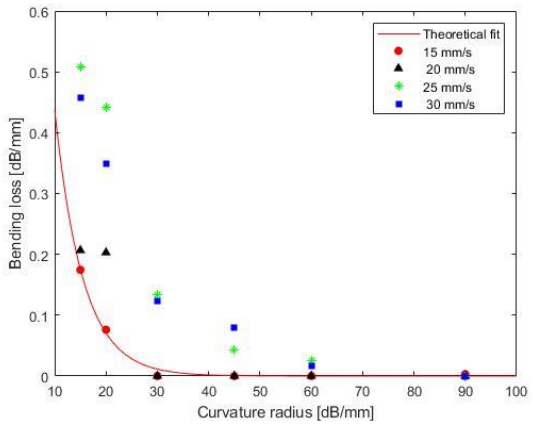


**Figure 3:** Bending Losses of waveguides written with different writing velocities as a function of the curvature radius. The red line represents the theoretical exponential fit [?].

We observed that for curvature radii greater than 45-mm, measured bending losses were negligible (see Figure 3).

.

## 3. Characterization of Directional Couplers

A directional coupler consists of two waveguides, both brought near to each other to a certain distance called the coupling distance *d*, for a given length called the coupling length *L*. This allows the power exchange between the two waveguides by evanescent-field interaction.

As a first test, we fabricated a series of directional couplers with a fixed coupling length *L* 2-mm and a coupling distance *d* that varies from 4µm to 10.5µm. Waveguides were written with 340 mW power and 15 mm/s of writing velocity at 6-um below the substrate surface. We have chosen to fabricate the directional couplers with a bending radius of $R = 45$ mm in order to deal with this trade-off. The transmissivity of the directional coupler composed of identical waveguides is expressed theoretically by the following formula:

$$T = sin^2(kz + \Phi) \qquad (3)$$

where  is the coupling coefficient, Φ is a term that accounts for the extra coupling occurring in the curving part.

We computed the experimental transmissivity of the directional couplers as:

$$T = \frac{P_2}{P_1 + P_2} \qquad (4)$$

Where *P*1 and *P*2 are the power values measured at the output of the first and second waveguides respectively, which light is coupled into the first one.

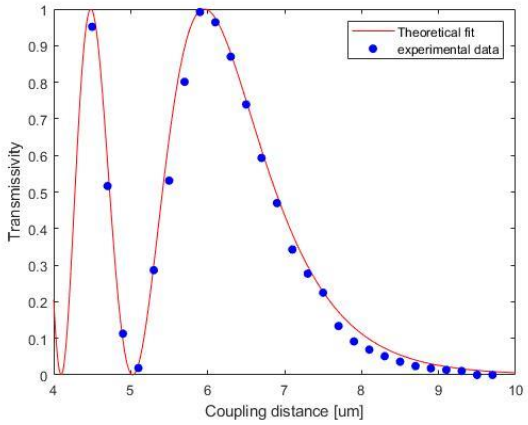


**Figure 4:** the transmissivity as function of the coupling distance *d*. The red line represents the theoretical fit.

The observations of the experimental data are plotted in Figure 4. We fitted Equation (3), considering an exponential decreasing coupling coefficient with the distance $k = k(d) = k_0 e^{\frac{d}{d_0}}$.

The theoretical model and the experimental data show good agreement, which attests to the quality of the waveguides and the stability of the directional couplers. Moreover, by further using Equation (3), we could retrieve the coupling coefficient *k* plotted in Figure (5).

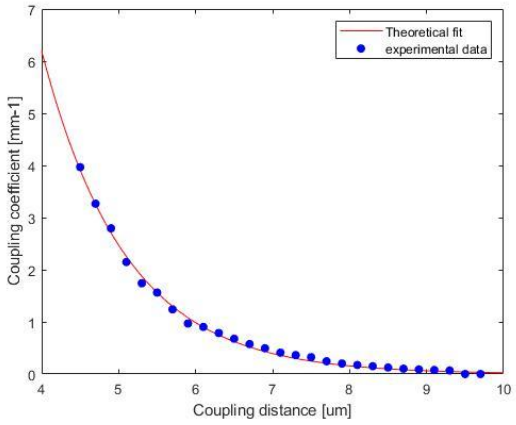


**Figure 5:** The coupling coefficient k as function of the coupling distance $d$. The red line represents an exponential fit.

As a further analysis, we experimentally explored the waveguide detuning using directional couplers. The transmissivity of directional couplers with unidentical arms is theoretically given by:

$$T = \frac{1}{1+\left(\frac{\Delta\beta}{2k}\right)^2} sin^2\left(kL\left(\sqrt{1+\left(\frac{\Delta\beta}{2k}\right)^2}\right)+\Phi\right) \qquad (5)$$

Where $\Delta\beta$ represents the detuning between the arms of the directional couplers

We fabricated a set of directional couplers with a fixed coupling distance $d = 6$ μm and a coupling length of $L = 3.35$ mm. In this devices we fabricated unidentical arms of directional coupler by varying the writing velocity of one arm from 15 mm/s to 30 mm/s, where the other arm is fabricated with a fixed writing velocity of 15 $mm/s$.

The experimental transmissivity of the directional coupler is plotted as function of the writing velocity difference $\Delta V$ between the arms of the directional couplers in Figure (6).

The detuning factor $\Delta\beta$ could be written as a function of the writing velocities of the directional coupler arms as follows:

$$\Delta\beta = C|V_1 - V_2| = C\,\Delta V \qquad (6)$$

Where $C$ is a coefficient that depends on the characteristics of the waveguides, $Vi$ represents the writing velocity of the $i$-th.

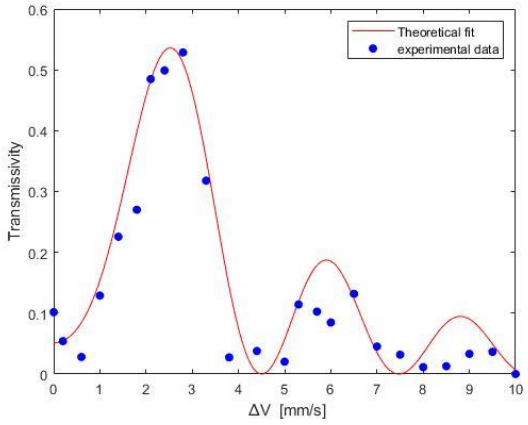


**Figure 6:** The transmissivity of the directional couplers as a function of the writing velocities difference of the two arms $\Delta V$. The red line represents the theoretical fit.

Data of Figure (5) are fitted with $k = 1.15mm^{-1}$ inserted in Eq (5), assuming that Δβ follows Eq(6) as retrieves for couplers with the same geometry, from another experiment. From the theoretical fitting the coefficient value is retrieved $C = 0.40 \pm 0.01\ mm{-}2s$. By using these information, we can proceed with the design of the final device.

The observations of the experimental data and the theoretical model (Eq 5) showed good agreement, which proves that the writing velocity is a strong parameter to detune the waveguides of the directional coupler.

## 4. Final Devices Optimization

Final devices consist of eight arms (single mode waveguides) placed at the vertices of an octagonal cross section following the layout shown in Figure (7).

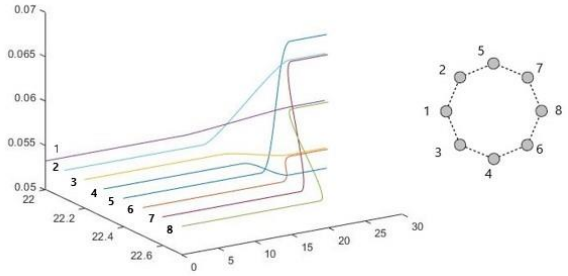

**Figure 7:** Geometrical configuration of the final device.

The waveguides are fabricated into two series with alternating writing velocity (say, the odd waveguides and the even waveguides). The even waveguides are fabricated with the so-called

reference writing velocity 15 mm/s, while the odd waveguides are fabricated with a different writing velocity. Two groups of devices were designed and fabricated to explore the waveguides coupling at the octagonal cross section configuration. First devices explore the influence of the waveguide characteristics, by varying the writing velocity difference $\Delta V$. Second devices explore the influence of the geometrical shape of the octagonal cross section, by varying the interaction distance d that tunes the coupling coefficient $k$.

As first group, four different devices were fabricated, having a fixed interaction length $L$=2$mm$ at the region of our interest and a fixed interaction distance $d$ = 6.6 μm that results from a fixed radius $R$ = 10 μm of the octagonal shape. The odd waveguides of the devices were all fabricated with the reference writing velocity (15 mm/s), Where the writing velocity of the even waveguides was different for each device (having 15, 19, 22, and 25 mm/s).

A second set of devices consists of seven different devices, having a fixed interaction length $L = 2mm$ at the region of our interest and a fixed writing velocity difference $\Delta V = 10$ mm/s between the even and odd waveguides. The interaction distance d between the waveguides at the vertices of the octagonal shape varies from 7.2 μm to 6 μm. As a result, the coupling coefficient is changing as well.

Characterization of the device performance is passed on a figure of merit that represents the ratio of power transmitted to the other arms, when light is inserted in a given input:

$$\text{Figure of merit} = \frac{\sum_{i=1}^{8} P_{out,i} - P_{out,j}}{\sum_{i=1}^{8} P_{out,i}} \qquad (7)$$

Where $j$ is the index of the input arm, $i$ is the index of the output arm, and $P_{out}$ represents the measured output power.

To perform the measurements, modes of the waveguide in the octagonal shape were imaged with a CCD making sure that the intensities of each mode profile do not saturate the sensitive pixels.

The devices are characterized by entering in three inputs (waveguide 2, 3, and 4). An example of image acquired with the CCD camera is reported in Fig 7.

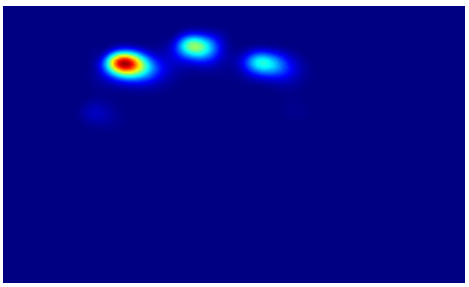

**Figure 7:** An image of the device output acquired with a CCD camera

The peak intensity's value of each mode of the acquired images was measured. The extracted values from each arm were used to calculate the figure of merit following Equation (7). The characterization is performed over three different waveguides for the two groups of devices, and results are reported in figure 8.

We note that figure of merit decreases with increasing the writing velocity difference ΔV, or increasing the interaction distance increased $d$. It is clear that the figure of merit is different for each arm. This inconsistency may appear due to the difference in the coupling between waveguides in the octagonal cross-section.

**A)**

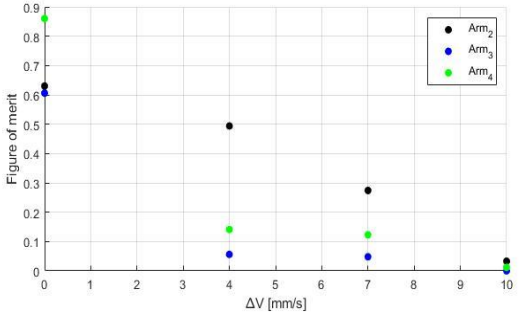


**B)**

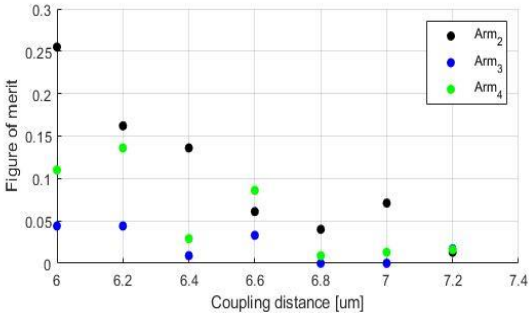


**Figure 8**: The figure of merit. (a) As a function of the writing velocity difference $\Delta V$. (b) As a function of the interaction distance d. Three waveguides of our device were characterized.

## 5. Conclusions

We reported and discussed a device that transforms eight waveguides from a planar configuration to an octagonal cross-section, where keeping good coupling among neighbouring waveguides. The waveguides are placed at the vertices of regular octagon. The device was fabricated by exploiting the unique three-dimensional capabilities of femtosecond laser micromachining. The device consists of single-mode optical waveguides working at 808 nm wavelength. Laser writing parameters were experimentally optimized to obtain low propagation loss (0.5 dB/cm), good coupling with optical fibres less than 0.1dB coupling loss and reasonable curvature radii (negligible additional loss for $R > 45$mm).

In the final device, we demonstrated that more than 95% of the input power remained in the same waveguide while the interaction distance was as low as 6.6 μm between the waveguides.
Future work could be devoted to controlling the coupling behaviours of the device's arms at different depths, as a function of the coupling angle to improve the device symmetry.
A full device to convert the encoded qubits into OAM encoded ones could be realized by combining the results of this thesis with the results of the discrete Fourier transformation and thermal shifter devices.

## References

[1]. Cozzolino, D., Da Lio, B., Bacco, D., & Oxenløwe, L. K. (2019). High-dimensional quantum communication: benefits, progress, and future challenges. Advanced Quantum Technologies, 2(12), 1900038.

[2]. Erhard, M., Fickler, R., Krenn, M., & Zeilinger, A. (2018). Twisted photons: new quantum perspectives in high dimensions. Light: Science & Applications, 7(3), 17146-17146.

[3]. Guan, B., Scott, R. P., Qin, C., Fontaine, N. K., Su, T., Ferrari, C., ... & Yoo, S. J. B. (2014). Free-space coherent optical communication with orbital angular, momentum multiplexing/demultiplexing using a hybrid 3D photonic integrated circuit. Optics express, 22(1), 145-156

[4]. Padgett, M. J. (2017). Orbital angular momentum 25 years on. Optics express, 25(10), 11265-11274.

[5]. Courtial, J., Dholakia, K., Allen, L., & Padgett, M. J. (1997). Gaussian beams with very high orbital angular momentum. Optics communications, 144(4-6), 210-213.

[6]. Crespi, A., & Bragheri, F. (2016). Projecting light beams with 3D waveguide arrays. Journal of Physics B: Atomic, Molecular and Optical Physics, 50(1), 014002.

[7]. Ceccarelli, F., Atzeni, S., Prencipe, A., Farinaro, R., & Osellame, R. (2019). Thermal phase shifters for femtosecond laser written photonic integrated circuits. Journal of Lightwave Technology, 37(17), 4275-4281.

[8]. Gattass, R. R., & Mazur, E. (2008). Femtosecond laser micromachining in transparent materials. Nature photonics, 2(4), 219-225.